tures in *En-1* homozygous mutants is a consequence of a lack of *En* gene function in the anterior neural folds between the one- and eight-somite stages. These results emphasize that early restricted gene expression reflects crucial genetic events that control regional brain development.

The KI approach has broad biological applications. With the appropriate choice of target locus, ectopic expression or gene transplant experiments can be carried out with a degree of control not afforded by the conventional transgenic approach. Such experiments are a necessary complement to elimination of gene function by mutagenesis, because loss of function may serve only to demonstrate that a developmental gene plays a role in the tissue in which it is expressed. Accurately regulated ectopic gene expression in vivo can generate viable mice exhibiting a gain-of-function phenotype (*12*). This can aid in determining the role of the gene in its normal environment or, as in these studies, can clarify the unique and overlapping functions of members of gene families. Because overlapping gene function is likely to be prevalent in mammals, such approaches are critical for determining the complete repertoire of functions of individual genes.

REFERENCES AND NOTES

1. C. Logan *et al.*, *Dev. Genet.* **13**, 345 (1992); A. L. Joyner and M. Hanks, *Semin. Dev. Biol.* **2**, 435 (1991).
2. A. P. McMahon, A. L. Joyner, A. Bradley, J. A. McMahon, *Cell* **69**, 581 (1992).
3. C. A. Davis, S. E. Noble-Topham, J. Rossant, A. L. Joyner, *Genes Dev.* **2**, 361 (1988); C. A. Davis and A. L. Joyner, *ibid.*, p. 1736; D. Davidson, E. Graham, C. Sime, R. Hill, *Development* **104**, 305 (1988).
4. A. L. Joyner, K. Herrup, B. A. Auerbach, C. A. Davis, J. Rossant, *Science* **251**, 1239 (1991); K. J. Millen, W. Wurst, K. Herrup, A. L. Joyner, *Development* **120**, 695 (1994).
5. W. Wurst, A. B. Auerbach, A. L. Joyner, *Development* **120**, 2065 (1994).
6. The *En-1* homologous sequences present in the KI targeting vectors (Fig. 1) were provided by a 4.2-kb Xba I–Apa I 5′ arm containing the *En-1* promoter, together with a 4.0-kb Cla I–Sac I 3′ arm (*5*), flanking either the coding sequence for *En-2* [1.2-kb Eco RI–Bg III fragment (*10*)] or *lacZ* [3.0-kb Eco RI fragment, containing a consensus eukaryotic ATG (S. Darling, unpublished data)] together with the PGK-Neo cassette (*5*). The vectors also carried the herpes simplex virus *TK* gene driven by the PGK promoter (*5*). *loxP* sites were inserted to flank the PGK-Neo cassette to allow CRE-mediated excision of this selectable marker in the event that expression of the targeted *En-1* locus was altered by its presence [R. Hoess, M. Zaise, N. Sternberg, *Proc. Natl. Acad. Sci. U.S.A.* **79**, 3398 (1982); P. C. Orban, D. Chui, J. Marth, *ibid.* **89**, 6861 (1992)]. R1 ES cells (2.5×10^7) [A. Nagy, J. Rossant, R. Nagy, N. W. Abromow, J. C. Roder, *ibid.* **90**, 8424 (1993)] were electroporated with 300 μg of linearized *En-2* or *lacZ* KI vector. After 8 to 9 days of selection in G418 and gancyclovir, approximately 200 double-resistant clones were picked from each experiment, amplified, and screened for the correct targeting event by Southern blot analysis (Fig. 1) [W. Wurst and A. L. Joyner, in *Gene Targeting, A Practical Approach*, A. L Joyner, Ed. (Oxford Univ. Press, Oxford, 1993), pp. 33–61]. Chimeric embryos from *lacZ*-targeted lines were generated by aggregation with diploid or tetraploid morulas, and mouse lines giving germline transmission of the *En-1*^{2ki} allele were established by diploid aggregation [A. Nagy and J. Rossant, *ibid.*, pp. 147–180].
7. C. Logan, W. K. Khoo, D. Cado, A. L. Joyner, *Development* **117**, 905 (1993).
8. M. Hanks and A. L. Joyner, unpublished observations.
9. C. A. Davis, D. P. Holmyard, K. J. Millen, A. L. Joyner, *Development* **111**, 287 (1991).
10. R. A. Conlon and J. Rossant, *ibid.* **116**, 357 (1992). The *En-2*–specific antisense probe was a 1.0-kb Cla I–Bg III fragment derived from the *En-2* complementary DNA (cDNA) [A. L. Joyner and G. R. Martin, *Genes Dev.* **1**, 29 (1987)].
11. X. Li and M. Noll, *Nature* **367**, 83 (1994).
12. M. Kessel, R. Balling, P. Gruss, *Cell* **61**, 301 (1990); M. H. Sham *et al.*, *ibid.* **72**, 183 (1993); M. Zhang *et al.*, *Development* **120**, 2431 (1994); J.Charité, W. De Graf, S. Shen, J. Deshchamps, *Cell* **78**, 589 (1994).

13. We dedicate this work to the memory of M. Breitman, for his enthusiasm, insight, and support. We also thank M. Kownacka and H. Park for technical assistance, S. Chu and K. Harpal for histology, and D. Fawcett and G. Fishell for critical comments on the manuscript. Funded by grants from the Medical Research Council (MRC) of Canada and Bristol-Myers Squibb. A.L.J. was a MRC Scientist and Howard Hughes International Scholar.

12 April 1995; accepted 15 June 1995

Role of the Ubiquitin-Proteasome Pathway in Regulating Abundance of the Cyclin-Dependent Kinase Inhibitor p27

Michele Pagano,* Sun W. Tam, Anne M. Theodoras, Peggy Beer-Romero, Giannino Del Sal, Vincent Chau, P. Renée Yew, Giulio F. Draetta, Mark Rolfe

The p27 mammalian cell cycle protein is an inhibitor of cyclin-dependent kinases. Both in vivo and in vitro, p27 was found to be degraded by the ubiquitin-proteasome pathway. The human ubiquitin-conjugating enzymes Ubc2 and Ubc3 were specifically involved in the ubiquitination of p27. Compared with proliferating cells, quiescent cells exhibited a smaller amount of p27 ubiquitinating activity, which accounted for the marked increase of p27 half-life measured in these cells. Thus, the abundance of p27 in cells is regulated by degradation. The specific proteolysis of p27 may represent a mechanism for regulating the activity of cyclin-dependent kinases.

The cyclin-dependent kinase inhibitor p27 (*1*) is present in maximal amounts during the quiescent (G_0) and prereplicative (G_1) phases of the mammalian cell cycle. The amount of p27 decreases as cells are induced to enter the cell cycle (*2–4*). Unlike all other mammalian cell cycle proteins studied so far, for which correlations have been found between the abundance of these proteins and changes in the amount of mRNA present (*5*), the decline in the amount of p27 occurs in the presence of constant amounts of mRNA and a constant rate of protein synthesis (*3, 4*). Thus, we investigated whether the intracellular regulation of p27 abundance involved the ubiquitin-proteasome pathway (*6*). We examined the effect of the peptide-aldehyde *N*-acetyl-leucinyl-leucinyl-norleucinal-*H* (LLnL), an inhibitor of the chymotryptic site on the proteasome (*7*), on the amount of cellular p27. As a control, we used the cysteine protease inhibitor L-*trans*-epoxysuccinic acid (E64).

Addition of LLnL, but not of E64 or a dimethyl sulfoxide (DMSO) vehicle, induced an accumulation of p27 protein after 60 min of treatment (Fig. 1A). In contrast, p21, another inhibitor of cyclin-dependent kinases, was not found to accumulate appreciably in LLnL-treated MG-63 cells, which lack the gene for the tumor suppressor p53. At later time points, we noticed that two antibodies to p27 that do not recognize the same epitope (*8*) both recognized a doublet with a relative molecular mass (M_r) of ~70,000. The p27 monoclonal antibody (mAb) also recognized a band of M_r ~100,000 in the extract from the 22-hour LLnL time point. To determine whether these bands contained ubiquitinated p27, we immunoprecipitated lysates from LLnL-treated cells with either anti-p27 or control antiserum and then immunoblotted them with a ubiquitin mAb. The M_r 70,000 doublet and a group of slower migrating bands were detected by the ubiquitin mAb exclusively in the anti-p27 immunoprecipitates (Fig. 1A). Immunoblotting with a control antibody of similar immunoprecipitates did not visualize any band (*8*).

M. Pagano, S. W. Tam, A. M. Theodoras, P. Beer-Romero, G. Del Sal, G. F. Draetta, M. Rolfe, Mitotix Inc., 1 Kendall Square, Building 600, Cambridge, MA 02139, USA.
V. Chau, Department of Pharmacology, Wayne State University, Detroit, MI 48201, USA.
P. R. Yew, Department of Cell Biology, Harvard Medical School, Boston, MA 02115, USA.
*To whom correspondence should be addressed.

When LLnL was introduced into cells by electroporation, the accumulation of ubiquitinated p27 was evident after 2 hours of treatment (Fig. 1B). We also used a murine *ts20TG*^{R} cell line bearing a temperature-sensitive mutation in the gene expressing the ubiquitin-activating enzyme E1 (9). In these cells, but not in their derivative H38-5 cells that had been engineered to express E1, p27 accumulated at the restrictive temperature (Fig. 1C).

We next investigated whether purified recombinant hexahistidine-tagged p27 (p27-his$_6$) was a substrate for ubiquitination in vitro in a rabbit reticulocyte lysate (RRL) system, which is an established source of ubiquitinating enzymes and proteasome complexes (*10*). Incubation of p27-his$_6$ with the RRL for as little as 1 min produced a ladder of bands that exceeded M_r 27,000, as visualized by immunoblotting with p27 mAb (Fig. 2A). The ladder of bands was not detected if the RRL was omitted from the reaction. No bands were recognized by anti-p27 if p27 was omitted, which demonstrated that the bands recognized by anti-p27 did not result from cross-reactivity with proteins present in the RRL (Fig. 2A). In time course experiments, the overall intensity of the bands decreased after a 3-hour incubation of p27-his$_6$ with the RRL (Fig. 2A). After 6 hours of incubation, the p27 band was further reduced and the ladder of bands had almost disappeared. The ubiquitination and degradation of p27 required adenosine triphosphate (ATP) hydrolysis. Because the RRL contains ATP, the addition of exogenous ATP did not change the reaction kinetics (Fig. 2A). Preincubation of the RRL with apyrase to hydrolyze ATP prevented the appearance of the slower migrating bands and inhibited p27 proteolysis. Addition of adenosine-5′-(γ-thio)-triphosphate (ATP-γ-S), a nonhydrolyzable ATP analog, led to a substantial reduction in the kinetics of p27 proteolysis (Fig. 2A). To demonstrate that the ladder of bands obtained in these reactions was the result of p27 ubiquitination, we added biotinylated ubiquitin to the degradation mix and, after the reaction was terminated, we repurified the p27-his$_6$. Ubiquitinated proteins were visualized by blotting with horseradish peroxidase (HRP)–conjugated streptavidin. Two major ubiquitin cross-reactive groups of bands comigrated with the bands identified by anti-p27 and were not detected in samples lacking bio-

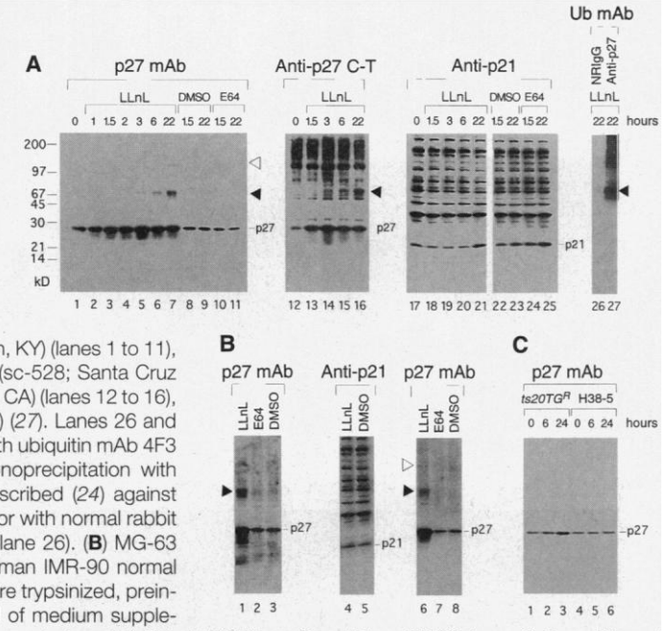

Fig. 1. Ubiquitination of p27 in vivo. (**A**) Human osteosarcoma MG-63 cells were treated for the indicated times with LLnL (lanes 2 to 7, 13 to 16, 18 to 21, 26, and 27), E64 (lanes 10, 11, 24, and 25), or DMSO (lanes 8, 9, 22, and 23). Lanes 1, 12, and 17: untreated cells. Cell lysates (*26*) were immunoblotted with p27 mAb (K25020; Transduction Laboratories, Lexington, KY) (lanes 1 to 11), anti-p27 C-terminus (C-T) (sc-528; Santa Cruz Biotechnology, Santa Cruz, CA) (lanes 12 to 16), or anti-p21 (lanes 17 to 25) (*27*). Lanes 26 and 27 show an immunoblot with ubiquitin mAb 4F3 (Ub mAb) (*28*) after immunoprecipitation with anti-p27 [generated as described (*24*) against purified p27-his$_6$] (lane 27) or with normal rabbit immunoglobulins (NRIgG) (lane 26). (**B**) MG-63 cells (lanes 1 to 5) and human IMR-90 normal fibroblasts (lanes 6 to 8) were trypsinized, preincubated for 1 hour in 1 ml of medium supplemented with 50 μM LLnL (lanes 1, 4, and 6), 50 μM E64 (lanes 2 and 7), or DMSO (lanes 3, 5, and 8), and electroporated in phosphate-buffered saline containing LLnL (1 μg/ml), E64 (1 μg/ml), or the equivalent amount of DMSO. Cells were incubated in the continued presence or absence of either peptide for an additional hour and were then lysed (*26*). Cell lysates were immunoblotted with p27 mAb (lanes 1 to 3 and 6 to 8) or anti-p21 (lanes 4 and 5). In (A) and (B), the solid arrowheads mark the M_r 70,000 doublet present only in cells treated with LLnL and recognized by anti-p27, p27 mAb, and ubiquitin mAb. The open arrowheads mark the M_r 100,000 band present only in cells treated with LLnL and recognized by p27 mAb. (**C**) Immunoblotting of cell lysates from *ts20TG*^{R} (lanes 1 to 3) or H38-5 cells (lanes 4 to 6). Cells were arrested in G_1 by serum deprivation and then incubated at the restrictive temperature for the indicated times.

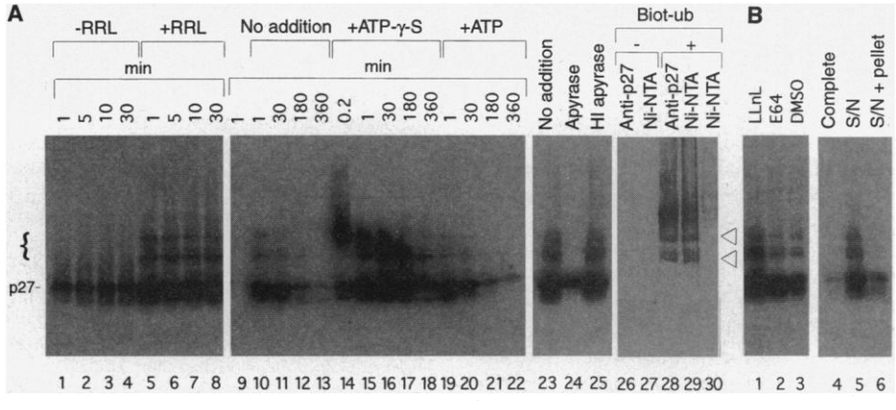

Fig. 2. In vitro ubiquitination and proteasome-mediated degradation of p27. (**A**) Purified p27 was incubated for the indicated times in the presence (lanes 5 to 8 and 10 to 25) or in the absence (lanes 1 to 4) of RRL. ATP (lanes 19 to 22) or ATP-γ-S (lanes 1 to 9 and 14 to 18) was added during the incubation (*25*); p27 was omitted in lane 9. Samples in lanes 24 and 25 were treated with apyrase (lane 24) or heat-inactivated (HI) apyrase (lane 25) and incubated at 37°C for 1 min. The reaction products in lanes 1 to 25 were analyzed by immunoblotting with p27 mAb. Samples in lanes 26 to 30 were incubated for 5 min at 37°C with ATP-γ-S in the absence (lanes 26 and 27) or in the presence (lanes 28 to 30) of 5 μM biotinylated ubiquitin (Biot-ub) and purified with anti-p27 (lanes 26 and 28) or affinity chromatography on Ni-NTA-agarose (Ni-NTA) (lanes 27, 29, and 30). Ubiquitinated proteins in lanes 26 to 30 were visualized by blotting with HRP-streptavidin (*25*). A slow migrating band in lanes 28 and 29, although less intense, was also present in a sample lacking p27 (lane 30) and is probably attributable to a ubiquitinated protein present in the RRL that binds unspecifically to the resin. The bracket marks a ladder of bands of M_r > 27,000 as visualized by immunoblotting with p27 mAb. The arrowheads mark the two groups of high molecular weight p27. (**B**) Purified recombinant p27 was incubated either for 2 hours with RRL in the presence of 50 μM LLnL (lane 1), 50 μM E64 (lane 2), or DMSO (lane 3), or for 6 hours with RRL (complete, lane 4), proteasome-depleted RRL [supernatant (S/N), lane 5], or proteasome-reconstituted RRL (supernatant + pellet, lane 6) (*25*). Samples were analyzed by immunoblotting with p27 mAb.

tinylated ubiquitin or p27 in the degradation mix (Fig. 2A). Finally, p27 ubiquitination was also observed with native in vitro–translated p27 (*8*). To demonstrate that the in vitro degradation of p27 required the proteasome, we added LLnL, E64, or DMSO to the degradation mix. LLnL, but not E64 or DMSO, inhibited p27 degradation and induced accumulation of p27-ubiquitinated forms (Fig. 2B). We also subjected the RRL to ultracentrifugation to eliminate the proteasome particles (*11*). Incubation of p27 with the proteasome-depleted supernatant did not result in p27 degradation, but upon readdition of the proteasome-rich pellet to the supernatant, p27 degradation was completely restored (Fig. 2B).

We tested whether the addition of purified recombinant human ubiquitin-conjugating enzymes (Ubcs or E2s) to the RRL altered the kinetics of the reaction (Fig. 3A). These enzymes included Ubc2 (Rad6) (*12*), Ubc3 (Cdc34) (*13*), Ubc4 (*14*), Ubc8 (*15*), an epidermal Ubc (Ubc-epi) (*16*), and Ubc9 (*17*). We also added HPV-18 E6, a known oncoprotein, which increases the rate of p53 degradation through the ubiquitin-proteasome pathway (*18*). Although Ubc2 and Ubc3 increased the rate of p27 turnover, the other proteins had no effect. Because of an increase in the rate of p27 ubiquitination compared to controls, samples to which Ubc2 or Ubc3 were added showed almost complete degradation of p27 after 2 to 3 hours of incubation. Incubation with Ubc3 specifically produced a smear of slower migrating bands. The difference observed with the different E2 enzymes was not the result of a difference in their ability to accept ubiquitin from E1, because all Ubcs were efficiently charged in reactions containing purified recombinant human E1 (Fig. 3B). Incubation of purified p27 with purified Ubc2 or Ubc3 generated a monoubiquitinated form of p27 (Fig. 3C). This reaction was dependent on ATP, ubiquitin, and E1. Because the reaction was somewhat inefficient and only a single ubiquitin molecule was added to p27, it seemed likely that efficient multiubiquitination of p27 requires additional factors that can be provided by the RRL. We mutated cysteines to serines in the active sites of human Ubc3 ($Cys^{88} \rightarrow Ser^{88}$), Ubc2 ($Cys^{93} \rightarrow Ser^{93}$), and Ubc4 ($Cys^{85} \rightarrow Ser^{85}$). The Ubc3 mutant also contained a $Leu^{97} \rightarrow Ser^{97}$ mutation, which has been shown to increase the dominant negative effect of yeast Cdc34 (*19*). Such E2 mutants were unable to accept activated ubiquitin from E1 (Fig. 3E) and efficiently competed for ubiquitination with their respective wild-type proteins in vitro (*8*). The rate of p27 degradation, which reflects the rate of its ubiquitination, was considerably slowed by the addition of Ubc3 mutant (Fig. 3D). Indeed, in samples to which Ubc3 mutant was added, the amount of p27 degradation after 12 hours was similar to that observed after 1 to 3 hours in control samples. The Ubc2

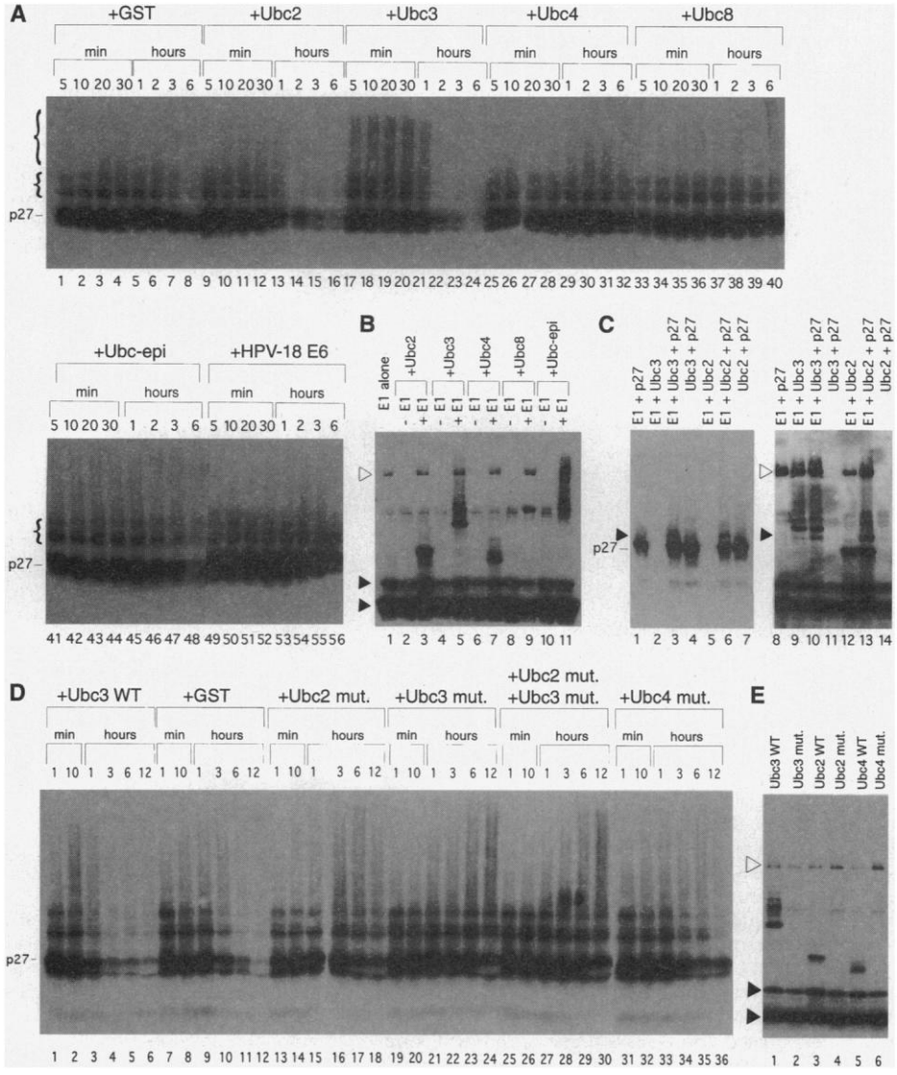

Fig. 3. Specific involvement of Ubc2 and Ubc3 in p27 turnover. (**A**) Purified recombinant p27 was incubated for the indicated times in the presence of RRL and ATP-γ-S with the addition of recombinant purified proteins as follows: GST (lanes 1 to 8), Ubc2 (lanes 9 to 16), Ubc3 (lanes 17 to 24), Ubc4 (lanes 25 to 32), Ubc8 (lanes 33 to 40), Ubc-epi (lanes 41 to 48), and HPV-18 E6 (lanes 49 to 56) (*25*). The reaction products were analyzed by immunoblotting with p27 mAb. The lower bracket marks a ladder of bands of M_r > 27,000; the upper bracket marks a smear of bands present only in samples with added Ubc3. (**B**) Ubc2 (lanes 2 and 3), Ubc3 (lanes 4 and 5), Ubc4 (lanes 6 and 7), Ubc8 (lanes 8 and 9), and Ubc-epi (lanes 10 and 11) were tested for the ability to form thioesters with biotinylated ubiquitin (*29*) in the presence (lanes 3, 5, 7, 9, and 11) or in the absence (lanes 2, 4, 6, 8, and 10) of E1. Lane 1 only contained E1. The open arrowhead marks the position of the E1-ubiquitin thioester; the solid arrowheads mark the positions of ubiquitin and dimers of ubiquitin. (**C**) Purified Ubc2 (lanes 5 to 7 and 12 to 14) and purified Ubc3 (lanes 2 to 4 and 9 to 11) were incubated in the presence (lanes 3, 4, 6, 7, 10, 11, 13, and 14) or in the absence (lanes 2, 5, 9, and 12) of purified p27 and in the absence (lanes 4, 7, 11, and 14) or in the presence (lanes 2, 3, 5, 6, 9, 10, 12, and 13) of purified E1. Lanes 1 and 8 only contained E1 and p27. Samples were analyzed by immunoblotting with p27 mAb (lanes 1 to 7) or HRP-streptavidin (lanes 8 to 14). The open arrowhead marks the position of the E1-ubiquitin thioester; the solid arrowheads mark the position of monoubiquitinated p27. (**D**) Purified recombinant p27 was incubated for the indicated times in the presence of RRL and ATP-γ-S with the addition of recombinant purified proteins as follows: Ubc3 (lanes 1 to 6), GST (lanes 7 to 12), Ubc2 mutant (lanes 13 to 18), Ubc3 mutant (lanes 19 to 24), Ubc2 and Ubc3 mutants (lanes 25 to 30), and Ubc4 mutant (lanes 31 to 36). The reaction products were analyzed as in (A). (**E**) Purified Ubc3 (lane 1), mutant Ubc3 (lane 2), Ubc2 (lane 3), mutant Ubc2 (lane 4), Ubc4 (lane 5), and mutant Ubc4 (lane 6) were tested for the ability to form thioesters with biotinylated ubiquitin (*29*). The open arrowhead marks the position of the E1-ubiquitin thioester; the solid arrowheads mark the positions of ubiquitin and dimers of ubiquitin.

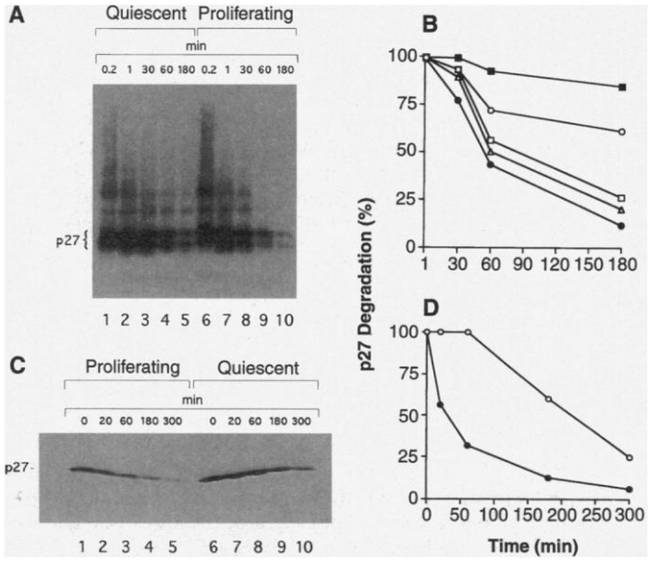

Fig. 4. Cell cycle regulation of p27 ubiquitinating activity and p27 half-life. (**A**) Purified recombinant p27 was incubated for the indicated times with extracts from quiescent (lanes 1 to 5) or proliferating (lanes 6 to 10) IMR-90 cells (*25*). The reaction products were analyzed by immunoblotting with p27 mAb. The bracket marks the nonubiquitinated forms of p27. (**B**) Profile of p27 degradation obtained by laser densitometry scanning of the two nonubiquitinated p27 bands (○, quiescent extracts; ●, proliferating extracts; □, quiescent extracts with the addition of recombinant purified Ubc2; △, quiescent extracts with the addition of recombinant purified Ubc3; ■, proliferating extracts with the addition of recombinant purified Ubc2 and Ubc3 mutants). (**C**) Pulse-chase analysis of the turnover rate of p27 in proliferating and quiescent cells. Immunoprecipitations of p27 from asynchronous growing cells (lanes 1 to 5) and cells arrested by serum deprivation (lanes 6 to 10) were performed with anti-p27 C-T. Cells were labeled with [^{35}S]methionine and [^{35}S]cysteine for 1 hour and then chased with medium for the indicated times. (**D**) Profile of p27 half-life obtained by laser densitometry scanning of the p27 bands shown in (C) (○, quiescent cells; ●, proliferating cells).

mutant had a less pronounced effect than did the Ubc3 mutant. Addition of both Ubc2 and Ubc3 mutant proteins had the same effect as the Ubc3 mutant protein alone. The Ubc4 mutant had no effect on p27 turnover.

We also used extracts from normal human fibroblasts as a source of ubiquitinating enzymes and proteasomes. Using such extracts, we confirmed that p27 degradation required an active proteasome (*8*). We found that extracts from proliferating cells contained more p27 ubiquitinating activity and degraded p27 faster than did extracts from quiescent cells (Fig. 4, A and B). Addition of dominant negative Ubc2-Ubc3 proteins to the proliferating fibroblast lysate caused a marked slowing of p27 degradation (Fig. 4B). Conversely, addition of purified Ubc2 or Ubc3 stimulated p27 degradation in quiescent cells (Fig. 4B). Given that the rate of synthesis of p27 does not change between quiescent and proliferating cells (*4*), this difference in degradation rates is likely to account for the change in the amount of protein. Pulse-chase analysis of the turnover rate of p27 demonstrated that the half-life of p27 in growing cells is one-sixth as long as its half-life in quiescent cells (Fig. 4, C and D).

Our findings show that p27 was degraded by the ubiquitin pathway in both normal and transformed mammalian cells and that, compared with proliferating cells, quiescent cells exhibited a smaller amount of p27 ubiquitinating activity, which accounts for the longer half-life measured in these cells. The ubiquitin-conjugating enzymes Ubc2 and Ubc3 were specifically involved in p27 ubiquitination, consistent with the fact that cell cycle arrest in G_1 occurs in *Saccharomyces cerevisiae* Cdc34 mutants following accumulation of $p40^{Sic1}$ (a yeast cyclin-dependent kinase inhibitor) (*20*). We propose that, in response to growth factor withdrawal, an increase in the amount of p27 is brought about by the inactivation of the ubiquitin-proteolytic system. In turn, p27 accumulation promotes cell cycle arrest.

REFERENCES AND NOTES

1. S. Elledge and W. Harper, *Curr. Opin. Cell Biol.* **6**, 847 (1994); C. Sherr and J. Roberts, *Genes Dev.* **9**, 1149 (1995).
2. E. J. Firpo *et al.*, *Mol. Cell. Biol.* **14**, 4889 (1994); J. Kato *et al.*, *Cell* **79**, 487 (1994); J. Nourse *et al.*, *Nature* **372**, 570 (1994); J. Slingerland *et al.*, *Mol. Cell. Biol.* **14**, 3683 (1994).
3. O. Halevy *et al.*, *Science* **267**, 1018 (1995).
4. S. W. Tam, A. M. Theodoras, G. F. Draetta, M. Pagano, unpublished data.
5. A. Murray and T. Hunt, *The Cell Cycle: An Introduction* (Freeman, New York, 1993).
6. S. Jentsch, *Annu. Rev. Genet.* **26**, 179 (1992); A. Ciechanover, *Cell* **79**, 13 (1994); M. Hochstrasser, *Curr. Opin. Cell Biol.* **7**, 215 (1995).
7. V. Palombella, O. Rando, A. Goldberg, T. Maniatis, *Cell* **78**, 773 (1994); K. Rock *et al.*, *ibid.*, p. 761.
8. M. Pagano, unpublished data.
9. D. Chowdary, J. Dermody, K. Jha, H. Ozer, *Mol. Cell. Biol.* **14**, 1997 (1994).
10. A. Hershko, *J. Biol. Chem.* **263**, 15237 (1988); A. Goldberg and K. Rock, *Nature* **357**, 375 (1992).
11. A. Hedge, A. Goldberg, J. Schwartz, *Proc. Natl. Acad. Sci. U.S.A.* **90**, 7436 (1993).
12. M. Koken *et al.*, *ibid.* **88**, 8865 (1991).
13. S. Plon *et al.*, *ibid.* **90**, 10484 (1993).
14. M. Rolfe *et al.*, *ibid.* **92**, 3264 (1995).
15. P. Kaiser *et al.*, *J. Biol. Chem.* **269**, 8797 (1994).
16. Z. Liu *et al.*, *ibid.* **267**, 15829 (1992).
17. M. Pagano, G. Draetta, V. Berlin, unpublished data.
18. M. Scheffner *et al.*, *Cell* **63**, 1129 (1990); B. Werness *et al.*, *Science* **248**, 76 (1990).
19. V. Chau, unpublished data.
20. E. Schwob *et al.*, *Cell* **79**, 233 (1994).
21. M. Pagano *et al.*, *Science* **255**, 1144 (1992).
22. F. C. Luca and J. V. Ruderman, *J. Cell Biol.* **109**, 1895 (1989).
23. T. Hunt *et al.*, *J. Mol. Biol.* **66**, 471 (1972).
24. M. Pagano, in *Cell Cycle—Materials and Methods*, M. Pagano, Ed. (Springer-Verlag, New York, 1995), chap. 24.
25. Purified p27-his$_6$ was incubated at 37°C for different times in 30 μl of degradation mix [final concentration 33% (v/v) RRL, 50 mM tris-HCl (pH 8.3), 5 mM $MgCl_2$, and 2 mM dithiothreitol], in the presence or absence of 0.5 mM ATP-γ-S and in the presence or absence of purified recombinant Ubc enzymes. In the original procedure, we also added 5 mM $CaCl_2$ because it was shown to help the in vitro degradation of *Xenopus* cyclins (*22*). We then verified that identical results were obtained with or without $CaCl_2$. All purified proteins in the degradation mix were used at ~1 μM. Ubiquitination of p27 was analyzed by immunoblotting with p27 mAb. In Fig. 4, the RRL was substituted by human cell extracts that were prepared as in (*23*) and added with ATP and an ATP regeneration system. In some cases, ubiquitinated p27 was detected by addition of 5 μM biotinylated ubiquitin to the degradation mix. After the reaction was stopped, p27 was purified with either Ni–nitrilotriacetic acid (NTA)–agarose (Invitrogen) or anti-p27 and blotted with HRP-streptavidin (Sigma) and a chemiluminescence (DuPont-NEN, Boston, MA) detection system. In some experiments, to remove the proteasome, the RRL was ultracentrifuged at 100,000*g* for 6 hours in the presence of 5 mM $MgCl_2$. In others, ATP was depleted from the RRL by treatment (20 min at 30°C) with apyrase [5 U/ml in 50 mM tris-HCl (pH 8.0), 4 mM $CaCl_2$, and 0.05% bovine serum albumin]. Ubc3-his$_6$, mutant Ubc3-his$_6$, and p27-his$_6$ were bacterially expressed and purified with Ni-NTA-agarose according to the manufacturer's instructions. Native Ubc2, Ubc4 (bacterially expressed), and E1 proteins (from baculovirus-infected cells) were purified as described (*14*). Glutathione-S-transferase (GST)–Ubc2 mutant, GST-Ubc4 mutant, GST-Ubc8, GST-Ubc9, and GST–Ubc-epi were bacterially expressed and purified with GSH-Sepharose (Pharmacia) according to the manufacturer's instructions.
26. Cell lysates were prepared as described (*21*) with a modified buffer consisting of 50 mM tris-HCl (pH 7.4), 0.25 M NaCl, 1% Triton X-100, 0.1% SDS, 0.5% deoxycholate, 1 mM EDTA, 50 mM NaF, 0.1 mM Na_3VO_4, 0.1 mM phenyl methyl sulfonyl fluoride, leupeptin (1 μg/ml), soybean trypsin inhibitor (10 μg/ml), L-1-chlor-3-(4-tosylamido)-4-phenyl-2-butanon (10 μg/ml), L-1-chlor-3-(4-tosylamido)-7-amino-2-heptanon-hydrochloride (10 μg/ml), aprotinin (1 μg/ml), and 10 mM *N*-ethylmaleimide.
27. H. Zhang *et al.*, *Genes Dev.* **8**, 1750 (1994).
28. L. A. Guarino *et al.*, *Cell* **80**, 301 (1995).
29. Purified proteins were incubated at 37°C for 30 min in 30 μl of ubiquitination mix [50 mM tris-HCl (pH 8.3), 5 mM $MgCl_2$, 1 mM dithiothreitol, 0.5 mM ATP-γ-S, and 5 μM biotinylated ubiquitin]. All purified proteins in the ubiquitination mix were used at ~1 μM. Samples were analyzed as in (*25*).

30. We thank I. Berdo for purifying native proteins, V. Berlin and C. Sherr for p27 complementary DNAs, J. Come for LLnL, L. A. Guarino for ubiquitin mAb 4F3, G. Hannon for anti-p21, H. Ozer for *ts20TG*^{R} and H38-5 cells, and A. Dutta and J. Roberts for useful criticisms. Supported in part by Human Science Frontier Program grant RG-496/93.

7 April 1995; accepted 30 May 1995